

**Omar F. Lutfy**

Control and Systems  
Engineering Department,  
University of Technology,  
Baghdad, Iraq  
[60157@uotechnology.edu.iq](mailto:60157@uotechnology.edu.iq)

**Alaa A. Abdul-Hamead**

Materials Engineering  
Department University of  
Technology, Baghdad, Iraq

Received on: 02/10/2017

Accepted on: 20/12/2017

## Intelligent Modeling of Metal Oxide Gas Sensor

**Abstract-** Due to the complexity of the gas detection process, traditional modeling techniques cannot provide accurate modeling performance to reproduce the behavior of this difficult process. In this paper, an intelligent modeling technique is utilized to develop an accurate model to represent the complex and nonlinear gas detection process. In particular, in this study nickel Oxide NiO gas sensor, which was specifically fabricated by a simple chemical spray pyrolysis technique. In the process, the nickel chloride hexahydrate salt was used at a concentration of (0.05 M) and a temperature of 350 °C. Because of this process, the thickness of NiO was 0.1 μm. Inspection was done using three different testing techniques; X-ray diffraction, scanning electron microscopy, and the sensitivity test of NiO for Methane gas CH<sub>4</sub> in the range of (0-500) ppm<sub>v</sub>. Inspection results show that the film was crystalline, has a cubic system, and without cracks or open pores. On the other hand, the sensitivity results were disparate and low in value within the considered range. From the real-time experiment described above, training samples were gathered to develop the desired process model. The considered modeling technique was based on exploiting the wavelet network (wavenet) to represent the nonlinear function of the nonlinear autoregressive with exogenous input (NARX) structure. In model development process, the experimental data were utilized as the training samples for the wavenet-based NARX model. As the modeling accuracy, the proposed wavenet-based NARX model attained a value of  $1.895 \times 10^{-12}$  for the root mean square of error (RMSE) criterion.

**Keywords-** gas sensor, metal oxides, nonlinear autoregressive with exogenous input (NARX), pollutant gases, spray pyrolysis, wavelet network.

**How to cite this article:** O.F. Lutfy, A.A. Abdul-Hamead, "Intelligent Modeling of Metal Oxide Gas Sensor," *Engineering and Technology Journal*, Vol. 36, Part A, No. 7, pp. 777-783, 2018.

### 1. Introduction

Owing to their low cost and high sensitivity, Metal Oxide gas sensors (MOX) are generally employed in gas detection processes. The applications of such sensors range from the alimentation and health examination fields to eco-friendly observations and system control problems. However, these MOX sensors suffer from specific limitations, such as the lack of selectivity, environmental influences, etc. Nanostructures of binary semiconducting oxides, like MgO, CuO and SnO<sub>2</sub>, have gained a huge attention due to their distinctive features and potential utilization in numerous problems, including photocatalysis, gas sensors, and solar cells [1]. Nevertheless, due to the advancement in the nanotechnology field, there is a vital necessity for especially developed semiconductors to superior match the characteristics of evolving materials. The Metal oxide semiconductor sensors are widespread for sensing poisonous and flammable gases at slight concentration levels because of their low manufacture prices, elevated sensitivity and extended-period stability. The

material attribute along with the size effect for the metal oxides were scouted for their chances in detection problems. Well-liked detection techniques uses variation in the electrical resistance of the MOX semiconductors created from ionosorption of gaseous kind on their superficies. The move of electrical charge which is induced by superficies responses defines the metal oxide resistance. In ambient temperature, the oxygen is ionosorbed on the surface of MOX, which leads to varying in the resistance resulted from a decrease or an increase in the surface electrons as a consequence of the adsorbed oxygen reacting with the sensate gas. For n-type semiconductor MOX, the resistance is increased in the presence of oxidizing gases like nitrogen monoxide (NO), nitrogen dioxide (NO<sub>2</sub>), ozone (O<sub>3</sub>), while the resistance is decreased with gases such as carbon monoxide (CO) and methane (CH<sub>4</sub>). The opposite is true for the p-type metal oxides. The variation amount in the electric resistance provides a straight work out of the concentration of the based on gas presence [2]. MOX conductometric gas sensors represent the

most widely applied and studied sensors which are designed for the control of inflammable and toxic gases in the industrial processes and the adjacent atmospheres. With a simple constructional structure, conductometric sensors consist of two elements, namely a sensitive conducting layer and contact electrodes. The working mechanism of a conductometric sensor is based on the change in resistance/conductivity of a sensitive layer under the effect of reactions (adsorption, chemical reactions, diffusion, catalysis), which take place on the sensing layer surface [3]. Various techniques can be utilized to synthesize the NiO, examples of these techniques include physical vapor deposition (PVD), chemical vapor deposition (CVD), flame pyrolysis, laser-ablation, arc discharge, sol-gel method, hydrothermal method, and solvo-thermal methods [4]. However, each of the above techniques has its own effect on the final MOX outside and so on the sensor sensitivity. Hence, researchers have considered intelligent modeling techniques in order to avoid the differences in sensitivity [5]. For instance, using artificial intelligence techniques, Divekar and Pawar [6] utilized PC-based multi sensors and a PIC microcontroller to achieve the gas identification process. In particular, they used film MOX gas sensors mercantile, namely; Figaro TGS 822, TGS 813, TGS 2600 and HANWEI MQ6 and MQ7. Various kinds of gases were considered, for example, methane, carbon monoxide and Liquid petroleum gas LPG (mixture largely of propane and butane and small amounts of other hydrocarbons gases) [7] at different temperatures. Using an artificial neural networks ANN model, the identification process was performed using the experimental data. Modeling performance was based on variation in different parameters, such as gas concentrations (only limit values near high 100, 400, 1000 ppm). The outcome was limited representing the ANN response for each sensor. Scott et al. made a review which covers aspects of analysis from sensor data to the electronic noses (e-noses) for the analysis of volatile organic compound. Different kinds of data analysis methods were utilized on the generated data. Subsequently, the focus was based on the employment of artificial intelligence approaches including neural networks and fuzzy logic systems for classification purposes and genetic algorithms for feature (sensor) selection [8]. In another work, Baha and Dibi [9] utilized a technique based on neural networks for smart gas sensors, which are in service in dynamical environments. They used industrial resistive gas sensors kind (TGS8xx, by Figaro Engineering).

They developed a model of neural network considering the relationship between the heat and the relative moisture on the sensing tip, besides the dependency on the nature of the gas in dynamical environments. The sensor's responses were linearized and compensated by the corrector. In particular, the method distinguished qualitatively and quantitatively seven gases at high concentration (50-5000 ppm) [9]. Balasubramanian et al. [10] studied neural network-integrated metal oxide-based artificial olfactory system for meat spoilage identification by TGS for Methane. Several signal processing methods were utilized to extract area-based features from the raw signals. The extracted features were used to develop radial basis function neural network classifiers. Absent appointment the gases amount related with sensor detections. Spinelle et al. [11] performed different methods of field calibration for low cost commercial sensors. The authors took into account a cluster of either the MOX or the electrochemical sensors for the nitrogen monoxide and the carbon monoxide together with the miniaturized infrared carbon dioxide sensors. The calibration has been performed in the first two weeks of assessment. Based on a five-months field experiment, the precision of each method has been assessed using different strategies, such as orthogonal regression, target diagram, measurement uncertainty and drifts over time of sensor predictions. In addition, the authors have considered if carbon monoxide sensors can achieve the Data Quality Objective (DQOs) of 25% of uncertainty set in the European Air Quality Directive for indicative methods. In all the above works, conventional ANNs were used to model the gas detection process. However, in recent years, wavelet neural networks (WNNs) have gained a wide popularity among researchers as more powerful universal approximators compared to conventional ANNs. The reason of this increased interest in WNNs is attributed to the fact that WNNs integrate both learning and generalization abilities of ANNs collectively with the localization property of wavelet transform. Accordingly, WNNs have been successfully employed to model various complex and nonlinear systems [12,13]. Nevertheless, the WNNs have not been utilized to model gas detection processes, in particular the fabricated nano structure MOX gas sensors. The main objectives of this work are to study a p-type nano gas sensor sensitivity for methane (pollutant gas in refinery application), and then to utilize the wavelet network as the nonlinear estimator in a NARX model to model the gas detection process.

The resulting model has achieved a highly accurate modeling result as will be demonstrated in the simulation results of this paper.

## 2. Materials and Methods

### I. Fabrication of the gas sensor

As a first step, an aqueous solution of nickel chloride hexahydrate ( $\text{NiCl}_2 \cdot 6\text{H}_2\text{O}$ ), with purities 99.9% was prepared. The concentration of this solution was (0.05 M), the acidity was  $\approx 6$  pH during spraying. In the spray pyrolysis technique, (Figure 1), prepared watery solutions have been atomized using a special nozzle glass sprayer at heated substrate glass which is fixed at thermostatic controlled hot plate heater. As a carrier gas, air was used to atomize the spray thawed utilizing an air compressor with a pressure of (8 Bar) and air flow rate of ( $8 \text{ cm}^3/\text{sec}$ ) at room temperature. Silicon p-type (111) substrate (0.6 mm thickness) is used temperature was maintained at  $350 \text{ }^\circ\text{C}$  throughout spraying, coating thickness was ( $0.1 \mu\text{m}$ ) tested by optical microscopy. Atomization rate was (3 nm/s) and (3 ml/min) for the rate of feeding. The distance between the spray nozzle and the collector has been maintained to be ( $15 \pm 1 \text{ cm}$ ). The spray solution volume was (25 ml), the number of spraying was (20) and the period between two attempt spraying was (6 sec). The following chemical reaction has resulted from the spray of the aqueous solution [14]:



The annealing was carried out under a vacuum of  $10^{-2} \text{ Pa}$  and took about 2 hours at a temperature of  $450 \text{ }^\circ\text{C}$ .

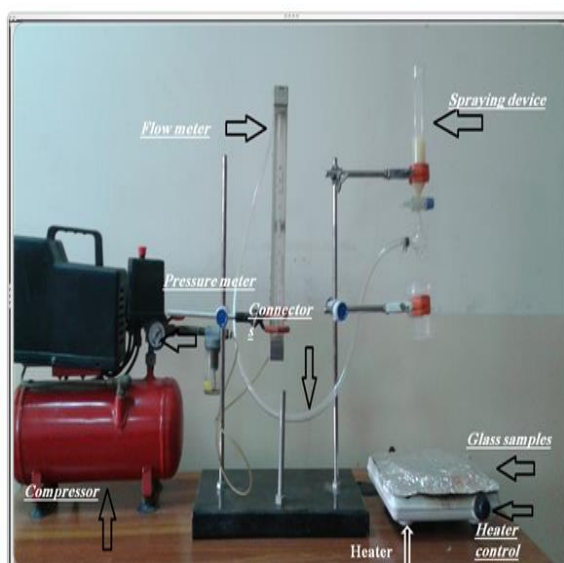


Figure 1: Spray pyrolysis system: flow meter, pressure meter, compressor, connector, spraying device, glass samples, heater and heater control

### II. Inspection of the Gas Sensor:

X-ray diffraction: It was taken by diffractometer type with radiation  $\text{CuK}\alpha$  ( $\lambda = 1.5406 \text{ \AA}$ ).

Scanning Electron Microscopy (SEM): This investigation was done by Electron Gun Tungsten heated filament, resolution 3 nm at 30kV, accelerating voltage 200 V to 30kV, chamber internal size: 160 mm (Japan), with Au coating for (20 sec).

### III. Experimental set-up of the gas sensor process

Gas-sensing testing was done by inserting the created sensor into a Hewlett-Packard Systems 5890 Series II GS device, as shown in Fig.2. In this system, an increment in  $\text{CH}_4$  gas from predicted gases was obtained. The gas-sensing property was determined for various concentrations of the  $\text{CH}_4$  gas within the range [0-500] ppm<sub>v</sub>. Figure 3 shows the electric circuit of gas sensor.

### IV. System identification procedure

The basic idea of the system identification process is to apply an appropriate input signal to the system in order to excite as much dynamic properties as possible. The response of the system to this input signal is then recorded. The resulting input-output data samples are then used to constitute the necessary model. To this end, by utilizing the fabricated gas sensor described in the previous section, the input-output data samples were obtained from the real-time experiment. In the obtained data samples, the input signal represents the concentration of the pollutant gas ( $\text{CH}_4$ ) which was in the range of [0-500] ppm, while the output signal represents the resistivity of the gas detector NiO/p-si. Figure 4 (a) shows the input signal and Figure 4 (b) depicts the related output signal resulted from the real-time experiment. To constitute the required model, the input-output data samples shown in Fig. 4 were used as the training data for the wavelet-based NARX model, which is described in the following section.



Figure2.  $\text{CH}_4$  gas sensor measurements setting.

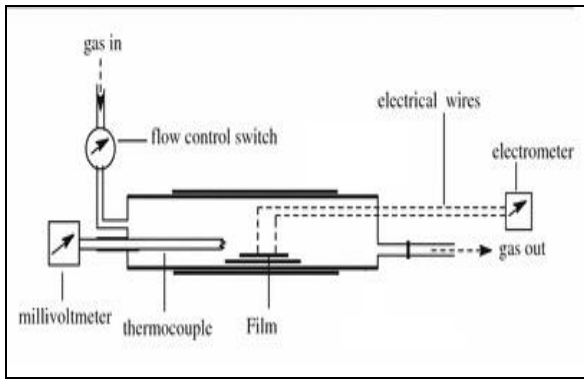


Figure 3: Electric Circuit of gas sensor.

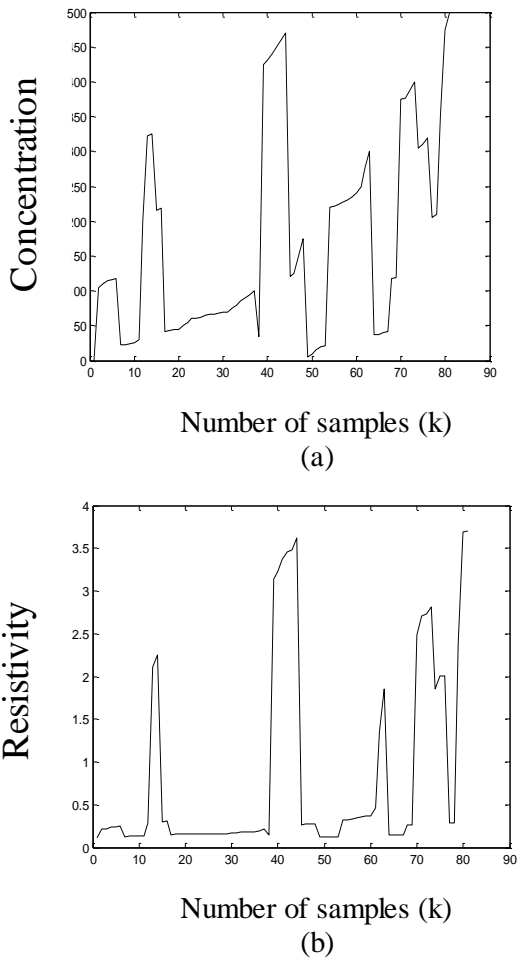


Figure 4. Input-output data resulted from the real-time experiment (a) input signal (concentration of the pollutant gas (CH<sub>4</sub>)) and (b) output response (resistivity of the gas detector NiO nano film).

V. The wavenet-based NARX model

To represent a nonlinear dynamical system, the NARX model employs a collection of previous output and input variables. These variables are known as the regressors of the model. In more details, the following equation is used to describe the NARX network [15,16]:

$$\hat{y}(k) = f[y(k-1), y(k-2), \dots, y(k-na), u(k-t_d), u(k-t_d-1), \dots, u(k-t_d-nb+1)], \quad (2)$$

where  $na$  is the number of past outputs,  $nb$  is the number of past inputs,  $t_d$  is the delay time,  $\hat{y}(k)$  is the estimated NARX output at time sample  $k$ ,  $y(k-1)$  and  $u(k-t_d)$  represent the system output and input, respectively, finally, the function  $f[\cdot]$  represents the NARX nonlinear function. In fact, there are several networks which can be used to represent the nonlinear function in Equation (2). However, after several simulation tests using various nonlinear networks, the wavenet network has accomplished the most accurate modeling performance in representing the gas detection process considered in this work. In order to better understand the output way of Equation (2) is calculated, let  $y=F(x)$ , in which  $y$  represents the scalar output of the NARX model and  $x$  represents a row vector of the regressors to the wavenet-based NARX network. Subsequently,  $F(x)$  can be expressed as follows [17, 18]:

$$F(x) = (x-r)PL + a_{s_1}f(b_{s_1}((x-r)Q - c_{s_1})) + \dots + a_{s_{ns}}f(b_{s_{ns}}((x-r)Q - c_{s_{ns}})) + a_{w_1}g(b_{w_1}((x-r)Q - c_{w_1})) + \dots + a_{w_{nw}}g(b_{w_{nw}}((x-r)Q - c_{w_{nw}})) + d \quad (3)$$

In Equation (3),  $r$  represents the mean value of the regressor vector  $x$ ,  $L$  is a linear vector,  $P$  and  $Q$  are projection matrices,  $d$  is an offset value,  $a_s$  and  $b_s$  ( $s=1, 2, \dots, ns$ ) represent scaling parameters,  $a_w$  and  $b_w$  ( $w=1, 2, \dots, nw$ ) represent the parameters of the wavelet terms,  $c_s$  ( $s=1, 2, \dots, ns$ ) represent vectors of the scaling terms,  $c_w$  ( $w=1, 2, \dots, nw$ ) represent vectors in the wavelet terms,  $f$  is the scaling function defined by  $f(x) = e^{-0.5xx^T}$ , and the function  $g$  is a wavelet

function of the type  $g(x) = (N_r - xx^T)e^{-0.5xx^T}$  where  $N_r$  is the regressor number in the NARX model. In order to determine the suitable settings of the modifiable parameters in Equation (2), the MATLAB function `nlrx` was used in this study [18]. As for the parameters of Equation (2), the following values were utilized:  $na = 5$ ,  $nb = 9$ ,  $td = 5$ . These values were adopted as they have achieved the best modeling performance for the system under consideration.

3. Results and Discussions

I. NiO nano film results

X-ray results: the result of X-ray diffraction, which represents precipitation of thin film, is demonstration in Figure 5. The XRD diffractogram pattern shows a correspond to the criterion (JCPDS card No.04-0835). Nickel oxide is a cubic system; hence, to determine the lattice

constant (a) by distance, we can use the following formula [19]:

$$\frac{1}{d^2} = \frac{h^2 + k^2 + l^2}{a^2} \quad (4)$$

where, d: is the distance between the adjacent planes in the set miller indices (hkl), λ : is the x-ray wavelength (Å). The lattice constant was about 4.176 Å. Moreover, the peaks are observed at 37.28° and 43.29° values of 2 θ° which correspond to (111) and (200) crystal planes, respectively. This result agrees with Sriram and A. Thayumanavan [20]. The average grain size (g) was about 40nm. This grain size was estimated using the following Scherrer's formula [20]:

$$g = \frac{0.94\lambda}{[B \cos \theta]} \quad (5)$$

where; B: Full Width at Half Maximum (Δ<sub>2θ</sub>) in radian and θ: bragg diffraction angle to the XRD peak (degree). The microstructure of the made NiO film is presented in Figure 6. SEM images demonstrate that the film is created fully and having a sticky nature with the Si substrate. The thickness was calculated by the mass method and it was less than 100 nm [21]. Crevice not founded also open pore observed on the surface. This broad stability domain can be attributed to the better NiCl<sub>2</sub> decomposition during the rest time, which was 6 seconds, used in the atomizer technique [22, 23]. Therefore, spray pyrolysis made the NiO film continuous, smooth, and with a completely close surface. The spray pyrolysis covers the Si substrate completely and creates areas of NiO without islands and conglomerates [24,25].

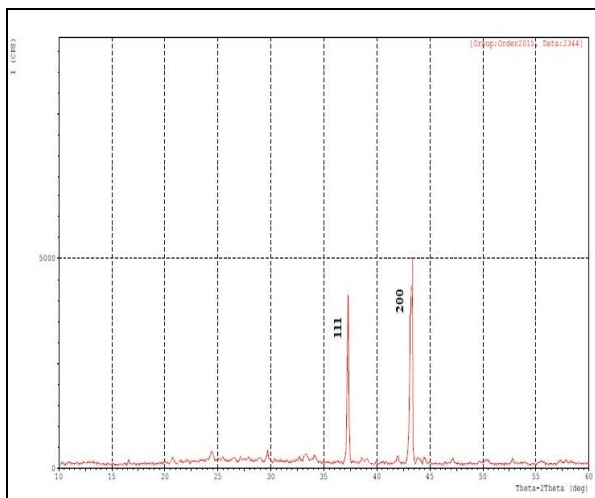


Figure 5: XRD diffractogram of NiO nano film.

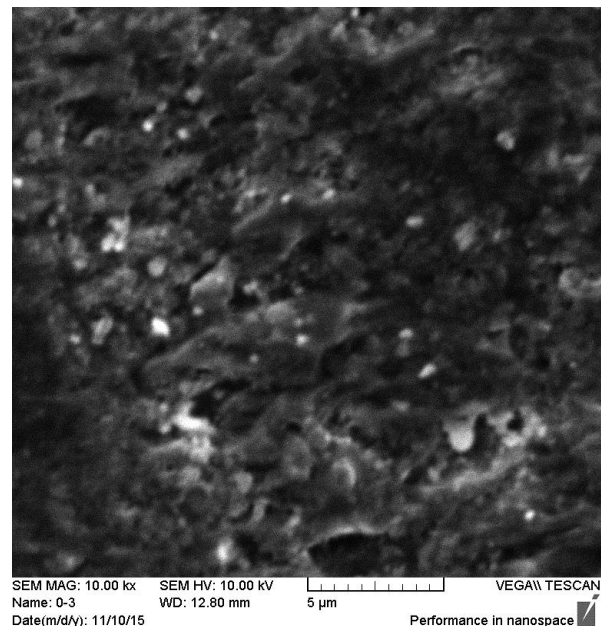


Figure 6: SEM result of NiO nano film.

## II. Simulation results

From the results of the CH<sub>4</sub> gas sensor, it was observed that the data collected from the experiment were random and do not follow a constant pattern. To handle this difficulty, these data were used to develop a suitable model that describes the gas detection behavior. To develop this model, the wavenet-based NARX model was used in this work. To demonstrate the modeling performance of the developed model, the root mean square of errors (RMSE) criterion is used in this work. In particular, the RMSE is defined as:

$$RMSE = \sqrt{\frac{1}{N} \sum_{k=1}^N (y(k) - \hat{y}(k))^2} \quad (6)$$

In the above equation, N represents the number of training data, y(k) and  $\hat{y}(k)$  signify the actual output of the system and the predicted output of the wavenet-based NARX model, respectively. Modeling result of wavenet-based NARX model representing the gas detection process is depicted in Figure 7, in which the solid line represents the actual system output while the ×-marks represent the model output. As can be obviously observed from Figure 7, the developed wavenet-based NARX model has done very well in reproducing the dynamics of the actual process. Specifically, the developed model has attained a RMSE of  $1.895 \times 10^{-12}$ . Error signal computed as the dissimilarity between the actual produce of the system with the estimated produce of the model is shown in Figure 8.

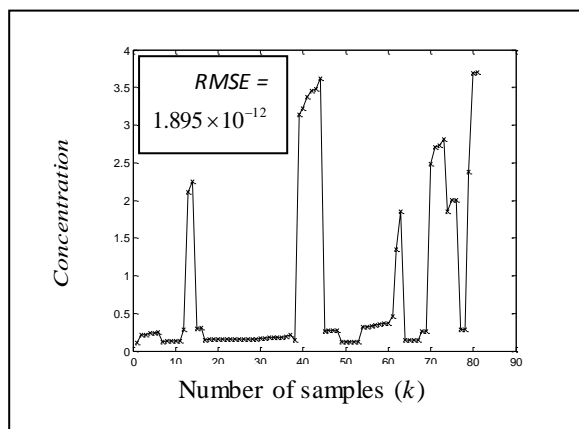


**Figure 7: Real response (solid line) and the developed model response (x-marks).**

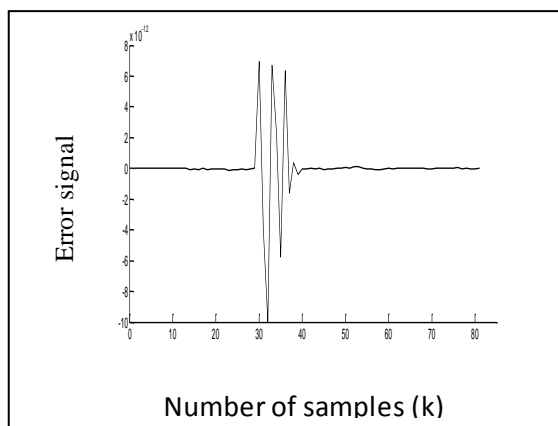


**Figure 8: Error signal between the real output and the estimated wavenet- based NARX model output.**

#### 4. Conclusion

Based on the NiO nano film inspection, it was demonstrated that fabricated pure films could be attained using spray pyrolysis technique from chloride precursor for gas sensor purposes.

To develop an accurate model representing the complex and nonlinear gas detection process, an intelligent modeling technique was employed using a NiO gas sensor. This sensor was specifically fabricated for this study by a simple chemical spray pyrolysis technique. At a concentration of 0.05 M and a temperature of 350 °C, the nickel chloride hexahydrate salt was used in the development process. In the development process, the nickel chloride hexahydrate salt was used at a concentration of (0.05 M) and a temperature of 350 °C. As a result of this process, the thickness of NiO was about 0.1 μm. Inspection was done by an XRD, SEM and sensitivity for Methane gas CH<sub>4</sub> in the range of (0-500) ppm<sub>v</sub>. Inspection results show that the film surface was crystalline, has a cubic system, and without cracks or open pores. Specifically, the considered modeling approach utilizes the wavelet network (wavenet) to represent the nonlinear function of

the considered network. To develop the model, experimental data samples were utilized as the training samples for the wavenet-based NARX model. These data samples were collected from a real-time experiment, which was conducted using a real physical gas sensor. This system was specifically fabricated for research purposes at the Materials Engineering Department, University of Technology. As the modeling accuracy, the suggested wavenet-based NARX model has accomplished RMSE of  $1.895 \times 10^{-12}$ . As opposed to other traditional modeling techniques, the proposed modeling approach is characterized by its simplicity and accuracy in representing the gas detection process under consideration. Therefore, the NiO films totally fulfill the desired characteristics, since they are very promising to be used in gas sensors.

#### References

- [1] W. Qi-Hui, L. Jing and S. Shi-Gang, "Nano SnO<sub>2</sub> gas sensors. Current Nanoscience," Vol. 6, pp.525-538, 2010.
- [2] S. Aarthy, W. Niti, Z.M. Myo Tay and D. Joydeep, "High-performance liquefied petroleum gas sensing based on nanostructures of zinc oxide and zinc stannate," Sensors and Actuators, Vol. 157, pp. 232-239, 2011.
- [3] G. Korotcenkov, V. Brinzari and K. C.Beong, "Conductometric gas sensors based on metal oxides modified with gold nanoparticles: a review," Microchim Acta, Vol. 183, pp.1033–1054, 2016.
- [4] D. Sreedhar, Y. Vinod Reddy and V. VasudevaRao, "Synthesis and analysis of ternary oxide nanomaterial for electro-thermal applications," Procedia Materials Science, Vol.10, pp.116 – 123, 2015.
- [5] J. Fonollosa, L. Fernández, A. Gutiérrez-Gálvez, R. Huerta and S. Marco, "Calibration transfer and drift counteraction in chemical sensor arrays using Direct Standardization," Sensors and Actuators B: Chemical, Vol. 236, 29, PP.1044–1053, 2016.
- [6] S.N. Divekar and S.N. Pawar, "PIC Microcontroller and PC based Multi Sensors Artificial Intelligent Technique for Gas Identification," International Journal of Computer Applications (0975 – 8887) Vol. 121 – No. 14, 2015.
- [7] M. Kojim, "The role of liquefied petroleum gas in reducing energy poverty," Extractive industrial for development series, Vol. 25, pp. 12, 2011.
- [8] S.M. Scott, D. James, and Z. Ali, "Data analysis for electronic nose systems," Microchim Acta Vol. 156, pp.183–207, 2016.
- [9] H. Baha and Z. Dibi, "A Novel Neural Network-Based Technique for Smart Gas Sensors Operating in a Dynamic Environment," Sensors, 9, 8944-8960, 2009.
- [10] S. Balasubramanian, S. Panigrahi, C.M. Logue, H. Gu and M. Marchello, "Neural networks-integrated

- metal oxide-based artificial olfactory system for meat spoilage identification,” *Journal of Food Engineering*, Vol. 91, pp.91–98, 2009.
- [11] L. Spinelle, M. Gerboles, M. Gabriella Villani and M. Alexandre, Fausto Bonavitacola, “Field calibration of a cluster of low-cost commercially available sensors for air quality monitoring,” *NO, CO and CO<sub>2</sub>, Sensors and Actuators Part B: Chemical*, B, Vol. 238, pp.706–715, 2017.
- [12] V.P. Androvitsaneas, A.K. Alexandridis, I.F. Gonos, G.D. Dounias and I. A. Stathopoulos, “Wavelet neural network methodology for ground resistance forecasting,” *Electric Power System Research*, Vol. 140, pp. 288-295, 2016.
- [13] M.R.G. Razin, and B.V. oosoghi, “Wavelet neural networks using particle swarm optimization training in modeling regional ionospheric total electron content,” *Journal of Atmospheric and Solar-Terrestrial Physics*, Vol. 149, 21-30, 2016.
- [14] Cleveland, Ohio, CRC Handbook of Chemistry and Physics, 1978.
- [15] H.K. Sahoo, P.K. Dash and N.P. Rath, “NARX model based nonlinear dynamic system identification using low complexity neural networks and robust H<sub>∞</sub> filter,” *Applied Soft Computing*, Vol.13,PP. 3324-3334, 2013.
- [16] A. Andalib and F. Atry, “Multi-step ahead forecasts for electricity prices using NARX: A new approach, a critical analysis of one-step ahead forecasts,” *Energy Conversion and Management*, Vol.50, PP. 739-747, 2009.
- [17] Q. Zhang, “Using wavelet network in nonparametric estimation,” *IEEE Transactions on Neural Networks*, 8, 2, 227-236, 1997.
- [18] Math Works. System Identification Toolbox™, User’s Guide. The MathWorks, Inc, 2014.
- [19] Y. Sirotnin and M. Shaskolskaya, “Fundamentals of Crystal Physics,” Mir Publishers, Moscow, 1982.
- [20] S. Sriram and A. Thayumanavan, “Structural, Optical and Electrical Properties of NiO Thin Films Prepared by Low Cost Spray Pyrolysis Technique”, *International Journal of Materials Science and Engineering* Vol. 1, pp.118-121, 2013.
- [21] R.P. Scott, “Measuring the Thickness of Thin Metal Films,” M.Sc. Thesis, Dep. of Physics and Astronomy, Brigham Young University, Idaho, United States, 2012.
- [22] B.A. Reguig, A. Khelil, L. Cattin, M. Morsli and J.C. Bernède, “Properties of NiO thin films deposited by intermittent spray pyrolysis process,” *Applied Surface Science*, Vol.253, pp. 4330–4334, 2017.
- [23] L. Cattin, B.A. Reguig, A. Khelil, M. Morsli, K. Benchouk and J.C. Bernède, “Properties of NiO thin films deposited by chemical spray pyrolysis using different precursor solutions,” *Applied Surface Science*, Vol. 254, pp. 5814–582, 2008.
- [24] F.A. Chyad, A.F. Hamood and L.S. Faiq, Effect of thermally sprayed ceramic coating on properties of low alloy steel, *Eng. & Tech. Journal*, Vol. 32, Part (A), No. 10, pp. 38-56, 2014.
- [25] F.M. Othman, A.A. Abdul-Hamead and A.S. Taeeh, Study of ZnO, SnO<sub>2</sub> and Compounds ZTO Structures Synthesized for Gas-Detection, *Eng. & Tech. Journal*, Vol. 33, Part (A), No. 6, pp. 2303-2312, 2015.